Astronomy & Astrophysics manuscript no. hess˙gk
December 21, 2011

Radio observations of the TeV source HESS J1943+213: a new case of a pulsar wind nebula?

K. É. Gabányi[1,2], G. Dubner[3], E. Giacani[3,4], Z. Paragi[5,1], Y. Pidopryhora[5], and S. Frey[2,1]

[1] MTA Research Group for Physical Geodesy and Geodynamics, PO Box 91, H-1521 Budapest, Hungary
[2] FÖMI Satellite Geodetic Observatory, PO Box 585, H-1592, Budapest, Hungary
e-mail: [gabanyik;frey]@sgo.fomi.hu
[3] Instituto de Astronomía y Física del Espacio (CONICET-UBA), CC 67, Suc. 28, 1428, Buenos Aires, Argentina
e-mail: [gdubner;egiacani]@iafe.uba.ar
[4] FADU, Universidad de Buenos Aires, Argentina
[5] Joint Institute for VLBI in Europe, Postbus 2, 7990 AA Dwingeloo, The Netherlands
e-mail: [zparagi;pidopryhora]@jive.nl

ABSTRACT

Context. Recently, the H.E.S.S. Collaboration discovered a very high energy gamma-ray point source close to the Galactic plane. They offered three possible explanations for the nature of the source: a gamma-ray binary, a pulsar wind nebula, or a BL Lacertae object. They concluded that the observations favoured an extreme BL Lacertae object interpretation.
Aims. We investigated the nature of the radio source reported as the counterpart of the very high energy gamma-ray source.
Methods. We performed high-resolution radio interferometric observations with the European Very Long Baseline Interferometry Network (EVN) at a frequency of 1.6 GHz on 2011 May 18. We also reanalysed archival 1.4-GHz radio continuum and HI spectral line data taken with the Very Large Array (VLA).
Results. The accurate position of the radio source, as observed with EVN, is $\sim 4''$ off from the one obtained in the NRAO VLA Sky Survey (NVSS). The new position is in excellent agreement with that of the proposed X-ray counterpart of the TeV source. The brightness temperature of the compact radio source is $\sim 8 \times 10^7$ K. From HI absorption data, a distance of about 11.5 ± 1.5 kpc can be inferred for this source. The large-scale HI data unveiled the presence of a shell-like feature with the radio/X-ray/TeV point source in its interior. We interpret this shell as the last vestige of a very old supernova that exploded in a tenuous environment created by the stellar wind of its massive stellar precursor.
Conclusions. The estimated brightness temperature of the radio point source counterpart of HESS J1943+213 is well below the value expected from the Doppler-boosted radio emission of a BL Lacertae object. This fact and the discovery of traces of a distant supernova explosion around the location of the TeV source lead us to conclude that the most likely origin of the high-energy emission is a remote pulsar wind nebula. If this scenario is true, then the HI shell around HESS J1943+213 may represent a population of hitherto missing Galactic supernova remnants.

Key words. Techniques: interferometric – Radio continuum: general – Radio lines: ISM – ISM: supernova remnants – Gamma rays: general – X-rays: individual: IGR J19443+2117

1. Introduction

The High Energy Stereoscopic System (H.E.S.S.) consists of four imaging atmospheric Cherenkov telescopes situated in the Khomas Highland of Namibia (Aharonian et al. 2006). The H.E.S.S. Collaboration has been surveying the Galactic plane for new very high energy (VHE, >100 GeV) gamma-ray sources. Recently Abramowski et al. (2011) reported the discovery of an unresolved VHE gamma-ray source close to the Galactic plane, HESS J1943+213. The conducted search for multi-wavelength counterparts revealed the presence of a hard X-ray source, observed by *INTEGRAL*, IGR J19443+2117, in the vicinity of the H.E.S.S. source. Landi et al. (2009) analyzed the data of the X-ray telescope onboard the *Swift* satellite to search for soft X-ray counterparts of three *INTEGRAL* sources, among them IGR J19443+2117. They concluded that they found firm soft X-ray localization of the source (SWIFT J1943.5+2120). Later, Tomsick et al. (2009) conducted *Chandra* X-ray observations of several *INTEGRAL* sources including IGR J19443+2117 to localize and measure their soft X-ray spectra. They concluded that IGR J19443+2117 is associated with the *Chandra* source CXOU J194356.2+211823 and the probability of spurious association is only 0.39 %. According to the precise *Chandra* measurement, the X-ray source is located 23″ away from HESS J1943+213 but still within the H.E.S.S. error circle, leading Abramowski et al. (2011) to identify the X-ray source with the H.E.S.S. source. All the proposed counterparts of HESS J1943+213 discussed by Abramowski et al. (2011) are located within the 68 % best-fit source position confidence level contour of HESS J1943+213 (see Fig. 6. in Abramowski et al. 2011).

In a search for a radio counterpart, a possible source is found in the U.S. National Radio Astronomy Observatory (NRAO) Very Large Array (VLA) Sky Survey (NVSS). The source, NVSS J194356+211826 (Condon et al. 1998) is located 24.″7 away from the H.E.S.S. position (still within the H.E.S.S. error circle) and 3.″5 away from the *Chandra* position. The *Chandra* source is outside the NVSS error circle.

Abramowski et al. (2011) discuss possible origins for HESS J1943+213, proposing that it can be either a gamma-ray binary, a pulsar wind nebula (PWN), or an active galactic nucleus (AGN). They conclude that observational facts favour the AGN interpretation, and suggest that HESS J1943+213 is an extreme, high-frequency peaked BL Lacertae object.

To better understand the nature of the VHE source, we conducted exploratory Very Long Baseline Interferometry (VLBI) continuum observations with the European VLBI Network (EVN) at 1.6 GHz frequency of NVSS J194356+211826 (hereafter J1943+2218). These observations permit to spatially resolve the radio source and to obtain its positional information with the precision of a few milli-arcseconds (mas). The high angular resolution study was complemented with the analysis of 1.4-GHz VLA radio continuum and neutral hydrogen emission and absorption data in an extended field around the VHE source. We describe the observations and data reduction in Sect. 2, and discuss our findings in Sect. 3 of this paper. Our conclusions are summarised in Sect. 4.

2. Observations and data reduction

The exploratory EVN observation of J1943+2118 took place on 2011 May 18. At a recording rate of up to 1024 Mbit s^{-1}, seven antennas participated in this e-VLBI experiment: Effelsberg (Germany), Jodrell Bank Lovell Telescope (UK), Medicina (Italy), Onsala (Sweden), Toruń (Poland), Hartebeesthoek (South Africa), and the phased array of the Westerbork Synthesis Radio Telescope (WSRT, The Netherlands). In an e-VLBI experiment (Szomoru 2008), the signals received at the remote radio telescopes are streamed over optical fibre networks directly to the central data processor for real-time correlation. The correlation took place at the EVN data processor in the Joint Institute for VLBI in Europe (JIVE), Dwingeloo, The Netherlands, with 2 s integration time. The observations lasted for 2 hours. Eight intermediate frequency channels (IFs) were used in both right and left circular polarisations. The total bandwidth was 128 MHz per polarisation.

The target source was observed in phase-reference mode to obtain precise relative positional information. It was crucial for strengthening the identification of the source, since there was a significant difference between the NVSS peak position and the *Chandra* position. The phase-reference calibrator source J1946+2300 is separated from the NVSS radio source by $1\overset{\circ}{.}77$ in the sky. Its coordinates in the current 2nd realisation of the International Celestial Reference Frame (ICRF2) are right ascension $\alpha = 19^{\rm h}46^{\rm m}6\overset{\rm s}{.}25140484$ and declination $\delta = +23^\circ0'4\overset{''}{.}4144890$ (Fey et al. 2009). The target–reference cycles of ∼5 min allowed us to spend ∼3.5 min on the target source in each cycle, thus providing almost 1.3 h total integration time on J1943+2118. The source position turned out to be offset from the phase centre position (taken from the NVSS catalogue) by ∼4″, but still within the undistorted field of view of the EVN.

The NRAO Astronomical Image Processing System (AIPS) was used for the data calibration in the standard way. We refer to Frey et al. (2008) for the details of the data reduction and imaging. The calibrated data were exported to the Caltech Difmap package for imaging. Phase self-calibration was only performed at the most sensitive antennas (Effelsberg, Jodrell Bank, WSRT). No amplitude self-calibration was applied. Finally, the longest baselines (from European telescopes to Hartebeesthoek) were excluded from the imaging because the signal was barely above the noise level due to the resolved nature of the source. The resulting image of J1943+2118 is displayed in Fig. 1.

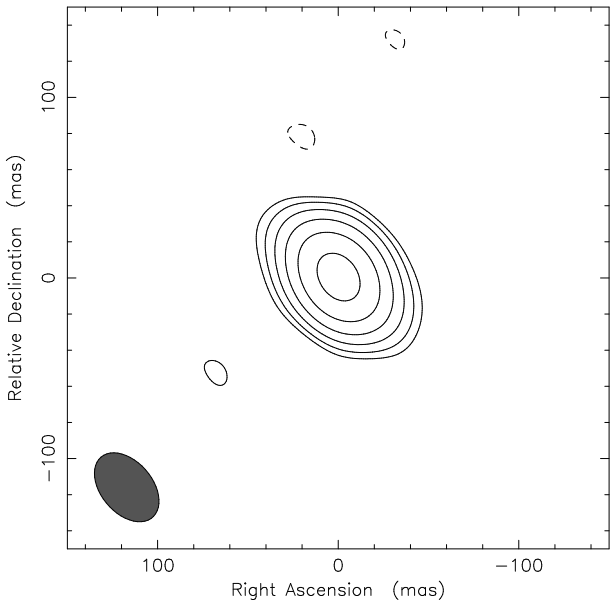

Fig. 1. 1.6-GHz EVN image of J1943+2118. The lowest contours are drawn at ±0.6 mJy/beam. The positive contour levels increase by a factor of 2. The peak brightness is 25.3 mJy/beam. The Gaussian restoring beam shown in the lower-left corner is 43.9 mas × 28.5 mas (full width at half maximum, FWHM) with major axis position angle $40\overset{\circ}{.}3$.

We also analysed archival VLA continuum data (project AH196, observing date 1985 September 30). These observations were taken from the region around our target source at 1.4 GHz, in the C configuration of the array, thus improving the angular resolution by a factor of three compared to the NVSS survey, which was performed with the most compact D configuration of the VLA.

The archival experiment AH196 included five different pointings covering a region of about $2\overset{\circ}{.}4\times1^\circ$ around our source of interest. The calibration was performed in AIPS, using 3C 48 as the primary flux density calibrator. We used Difmap to obtain the image shown in Fig. 2.

We also investigated the neutral hydrogen (HI) radio emission in a large field around the VHE source. To carry out this study, we made use of the data from the VLA Galactic Plane Survey (VGPS, Stil et al. 2006).

3. Results and discussion

3.1. Radio continuum: no blazar-like compact emission

The phase-referenced exploratory EVN observation provided accurate equatorial coordinates for J1943+2118: $\alpha = 19^{\rm h}43^{\rm m}56\overset{\rm s}{.}2372 \pm 0\overset{\rm s}{.}0001$ and $\delta = 21^\circ18'23\overset{''}{.}402 \pm 0\overset{''}{.}002$. This position agrees well, within uncertainties, with the coordinates of CXOU J194356.2+211823, the X-ray source proposed to be the counterpart of the H.E.S.S. point source (Abramowski et al. 2011). Therefore we can confirm that J1943+2118 is indeed the radio counterpart of CXOU J194356.2+211823 and consequently very likely to be associated with the VHE emission detected by H.E.S.S. It has to be noted that the EVN detection is $3\overset{''}{.}75$ off from the position given in the NVSS catalogue.

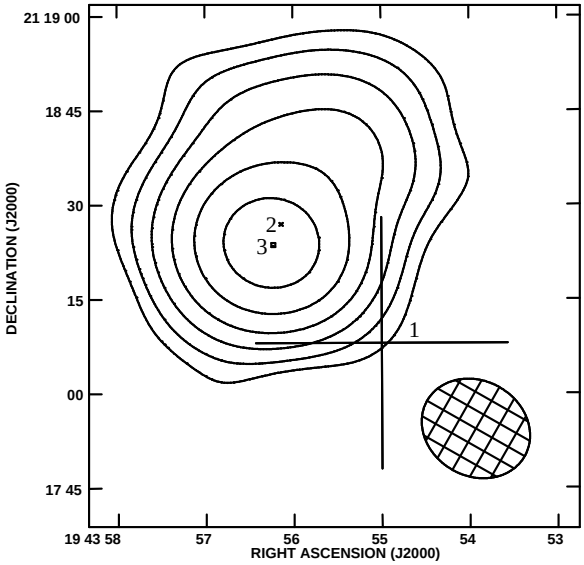

Fig. 2. 1.4-GHz VLA C-configuration image of J1943+2118. The peak brightness is 60 mJy/beam. The lowest contours are drawn at ±1.2 mJy/beam and the positive contour levels increase by a factor of 2. The Gaussian restoring beam shown in the lower-right corner is $17\farcs8 \times 15\farcs1$ with major axis position angle $60\fdg1$. Label number 1 indicates the TeV source position and its 90 % error measured by H.E.S.S. The NVSS source position and the position of the X-ray counterpart is labelled as number 2 and number 3, respectively. The sizes of the symbols represent the errors of the corresponding position measurement. The *Chandra* position coincides with the position of the radio source derived from our phase-referencing EVN observation. (The accuracy of the EVN position is superior to that of the X-ray, therefore it cannot be distinctively displayed in this figure.)

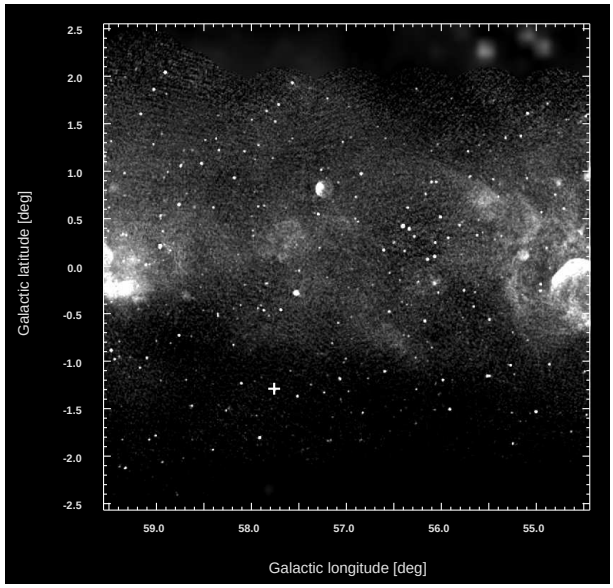

Fig. 3. Radio continuum emission at 1.4 GHz as taken from the VGPS (Stil et al. 2006). The white cross indicates the location of J1943+2118. Note that this map is presented in galactic coordinates.

We used the Difmap package to fit a circular Gaussian brightness distribution model component to the VLBI visibility data. The feature in our EVN image can be well described with a component of 31 mJy flux density and 15.8 mas angular size (full width at half maximum, FWHM). These values imply a brightness temperature of $T_{\rm B} = 7.9 \times 10^7$ K. Since J1943+2118 is very close to the Galactic plane (at about $-1\fdg3$ Galactic latitude), angular broadening caused by the intervening ionised interstellar matter can distort the image of a distant compact extragalactic radio source. According to the model of Cordes & Lazio (2002), the maximal amount of angular broadening of a point source in this direction at 1.6 GHz (at the frequency of our EVN observation) is expected to be 3.34 mas. However, even if we take this effect into account, the "de-broadened" source size remains quite large. The brightness temperature calculated using this "de-broadened" source size is still substantially lower than the intrinsic equipartition value estimated for relativistic compact jets ($\sim 5 \times 10^{10}$ K, Readhead 1994). Thus relativistic beaming most probably does not play a role in the appearance of this source.

The flux density recovered in our high-resolution EVN observation is only one-third of the value reported by NVSS at 1.4 GHz, (102.6±3.6) mJy. To investigate the discrepancy between the flux density values, we analysed the WSRT phased array data taken during our EVN experiment. The offset of the source position from the phase centre is a significant fraction of the synthesised beam of the phased array of the WSRT ($7\farcs8$ at 1.6 GHz) therefore the derived source characteristics should be used with caution. However, the obtained flux density value, ∼95 mJy, still agrees well with the value reported in the NVSS for J1943+2118. Thus, we can conclude that the high-resolution EVN observation resolved out significant portion of the large-scale structure of J1943+2118. This was confirmed with the archival VLA C-array data (see Fig. 2). According to those, the flux density of the source is (91±5) mJy, which agrees with the flux density values derived from the two other (the NVSS and the WSRT-only) lower-resolution data sets.

Additionally, the VLA C-array data revealed an elongated structure of J1943+2118 in the SE-NW direction. This shape can naturally explain why the NVSS position is ∼ 4″ off. In Fig. 2, label 2 indicates the NVSS position, while label 3 indicates the coinciding *Chandra* X-ray and EVN radio positions. The shift between points 2 and 3 is exactly in the direction of the source extension.

Finally, to gain insight into the field where HESS J1943+213 is located, and to search for possibly associated extended emission, we inspected the VGPS image of the radio continuum emission at 1.4 GHz in a 5°×5° area around the source position (Fig. 3). Essentially, it shows an almost empty field around J1943+2118 (whose location is indicated by a white cross in Fig. 3), with no trace of diffuse emission at the sensitivity of this survey. The reprocessed VLA C-array archival data confirm this picture, down to an rms noise level of 0.15 mJy/beam.

3.2. HI data: the distance and the associated features

With an angular resolution of 1′ and a sensitivity of 11 mJy/beam (2 K for a 1′ beam), the VGPS (Stil et al. 2006) is an adequate database to search for possible footprints of the event that resulted in the very high-energy emission detected by H.E.S.S. We have carried out an HI absorption study to constrain the distance to J1943+2118. Fig. 4 displays the HI profile traced towards the point source (top panel) and the absorption spectrum obtained from the subtraction of this profile from the average of four surrounding offset points (lower panel). From these spectra we can conclude that there is an absorption feature at $v \approx -16$ km s^{-1}, fol-

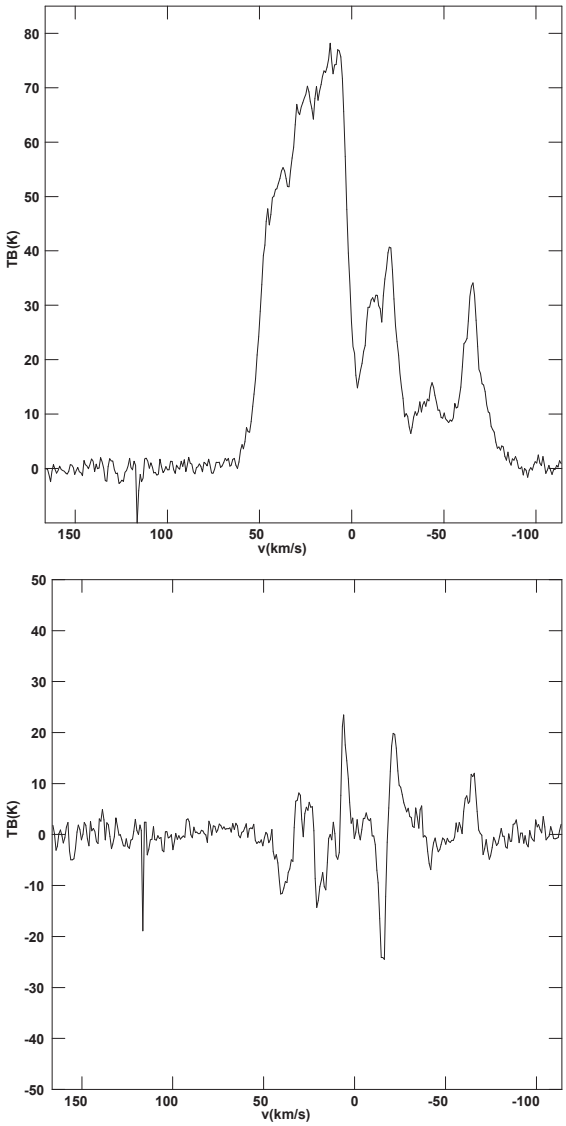

Fig. 4. Top panel: HI spectrum towards J1943+2118. Bottom panel: absorption HI spectrum obtained from the subtraction of the above profile from the average of four offset profiles.

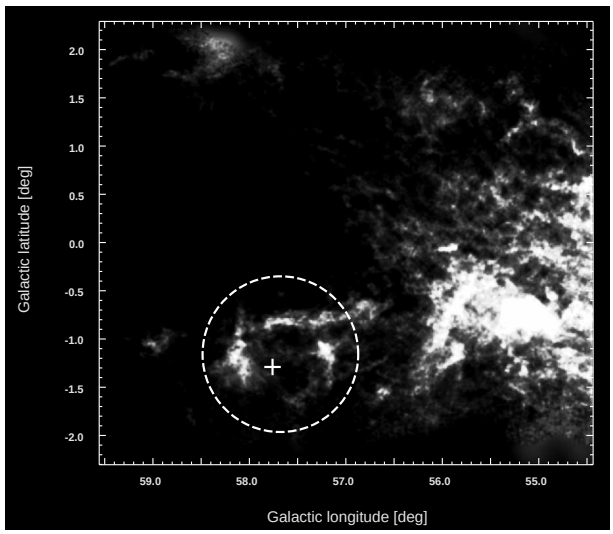

Fig. 5. HI emission distribution from VGPS, within the velocity range $+50\,\mathrm{km\,s^{-1}}$ to $+57\,\mathrm{km\,s^{-1}}$. The white cross shows the location of J1943+2118 and the white dashed circle marks up the location of the discovered HI shell. Note that this map is presented in galactic coordinates.

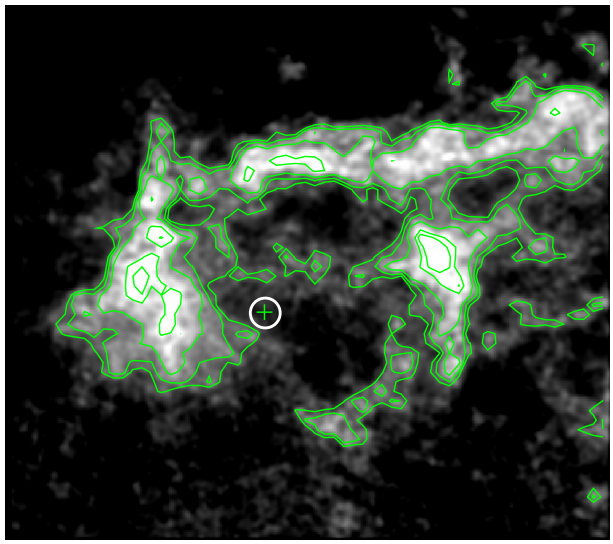

Fig. 6. A detailed view of the HI shell shown in Fig. 5. The cross shows the location of J1943+2118 and the circle is the 2′.8 confidence size of HESS J1943+213.

lowed by an emission feature peaking near $v{\approx}{-}50\,\mathrm{km\,s^{-1}}$. By applying a Galactic circular rotation model (Fich et al. 1989), we set tentative limits for the distance to J1943+2118, concluding that it is beyond 10 kpc (corresponding to the radial velocity $-16\,\mathrm{km\,s^{-1}}$) but closer than 13 kpc (corresponding to the radial velocity $-50\,\mathrm{km\,s^{-1}}$). In what follows we adopt as a compromise an intermediate distance of 11.5 kpc for J1943+2118. We note that the emission feature seen at $-50\,\mathrm{km\,s^{-1}}$ lies most probably in the warping region of the outer galaxy (Voskes & Burton 2006) further than J1943+2118 and does not seem to be related to it.

By inspecting the HI emission in the large 5°×5° field, across the whole observed velocity range between $-114\,\mathrm{km\,s^{-1}}$ and $+166\,\mathrm{km\,s^{-1}}$, we find that in all channel maps between radial velocity $v{\approx}{+}50\,\mathrm{km\,s^{-1}}$ and $v{\approx}{+}57\,\mathrm{km\,s^{-1}}$, a striking, almost complete shell-like feature surrounds the location of J1943+2118 (Fig. 5).

This HI shell, displayed in detail in Fig. 6, appears at a "forbidden" velocity for the expected rotational properties of the Galactic gaseous disk, since in this direction of the Galaxy (Galactic longitude $l{\sim}57°$) the maximum positive velocity (corresponding to the tangent point) is predicted to be about $+35\,\mathrm{km\,s^{-1}}$. This fact is not surprising. Recently Kang et al. (2010) discussed the presence of many faint, wing-like HI features at velocities beyond the boundaries allowed by Galactic rotation (what they call Forbidden-Velocity Wings, FVWs), and conclude that these features are the results of violent events, probably missing old Galactic supernova remnants (SNRs) which are invisible in other spectral regimes.

With this idea in mind, we investigated the characteristic physical parameters of the newly detected HI shell around J1943+2118. In Table 1 we summarise the observed and derived parameters of the HI shell (for the adopted distance of 11.5 kpc).

Table 1. Observed and derived parameters of the HI shell.

Geometrical centre:	
Equatorial coordinates	$\alpha = 19^h43^m23^s, \delta = +21°10'45''$
Galactic coordinates	$l = 57.^\circ6, b = -1.^\circ25$
Angular diameter	$1°$
Linear diameter	200 pc
Adopted systemic velocity	$-16\,\mathrm{km\,s^{-1}}$
Adopted central velocity	$+54\,\mathrm{km\,s^{-1}}$
Expansion velocity	$70\,\mathrm{km\,s^{-1}}$
HI mass	$6.4 \times 10^4\,\mathrm{M_\odot}$
Ambient density	$0.6\,\mathrm{cm^{-3}}$
Kinetic energy	1.6×10^{51} erg
Initial energy	1.6×10^{52} erg
Dynamic age	4×10^5 years

The central velocity was derived on the basis of the velocity of the central channel of the nine where the HI shell is clearly detected between $+50\,\mathrm{km\,s^{-1}}$ and $+57\,\mathrm{km\,s^{-1}}$. The expansion velocity is estimated by adding the $\sim 54\,\mathrm{km\,s^{-1}}$ at which the shell is seen, to the absolute value of the assumed systemic velocity of approximately $-16\,\mathrm{km\,s^{-1}}$, as suggested by the absorption study. We also searched for the expanding "caps" of the shell at the appropriate velocities, i. e. $(-16 - 70)\,\mathrm{km\,s^{-1}} = -86\,\mathrm{km\,s^{-1}}$. Even though quite faint, we found traces of the HI shell at a very close velocity value, $-81\,\mathrm{km\,s^{-1}}$. The HI mass was calculated by integrating all contributions within the shell across all the channels where the shell is present. The ambient density was derived by assuming that all the swept-up mass that forms the shell was initially uniformly distributed within a sphere of 200 pc diameter. The initial energy was calculated from the relation (Cioffi et al. 1988): $E_{\rm SN} = 6.8 \times 10^{43}\ n_0^{1.16}\ R_{\rm s}^{3.16}\ v_{\rm exp}^{1.35}\ \xi^{0.161}$ ergs, where ξ, the metallicity index, is adopted 0.2, corresponding to $d \approx 10$ kpc (Maciel & Quireza 1999). Finally, the dynamic age is calculated from the relation $t \sim 0.3 R_{\rm s}/v_{\rm exp}$.

All the observed and calculated parameters for this shell are completely analogous to those obtained by Koo et al. (2006), who conducted an HI study towards one of the FVWs, the structure FVW 190.2+1.1. They concluded that such parameters are only consistent with the HI shell being the last remnant of a supernova (SN) explosion that occurred in the outermost fringes of the Galaxy some 3×10^5 years ago, an SNR that is not seen in any other wavebands, and that represents the oldest type of SNRs, essentially invisible except via its HI line emission.

In our case, the observed HI shell might be the last vestige of an old, very energetic SN that exploded on the other side of the Galaxy, about 400 000 years ago, and is currently expanding in a tenuous interstellar gas. These facts explain the absence of radio continuum emission associated with this remnant. In this scenario, the sources detected in TeV, radio, and X-rays would be the emission from the PWN. For comparison, if the paradigmatic PWNe Crab and 3C 58 were located at a distance of 11.5 kpc, as the approximate distance of J1943+2118, their angular size in radio wavelengths would be of the order of $1.'2 \times 0.'8$ for Crab and $\sim 0.'8$ for 3C 58, in excellent concordance with the size of the elliptical structure of J1943+2118 as seen from the VLA observation. The size of the PWNe in X-rays is generally smaller than in radio due to the smaller synchrotron lifetimes of the higher-energy electrons (Slane et al. 2000), thus explaining why *Chandra* detected it as a point-like source. Besides, the radio spectral index -0.32 reported by Vollmer et al. (2010) for the NVSS point source coincident with J1943+2118 is compatible with the standard spectral indices of PWNe (between 0 and -0.3, Gaensler & Slane 2006).

However, one problem arises in this scenario. According to Mattana et al. (2009), the gamma-ray to X-ray flux ratio is proportional to the age of the PWN. The relatively low value of the flux ratio (0.04) of J1943+2118 implies that the nebula is only $\sim 10^3$ years old, more than hundred times younger than the age implied by the dynamics of the HI shell. This contradiction can be resolved if the HI shell was produced by the stellar wind of the massive supernova progenitor. As the SNR expanded in a previously evacuated cavity, the ambient density to create the SNR shell was very low and it is natural that the SNR remained undetected. Such HI bubbles are common features around massive early-type stars which eventually end their lives exploding as SNe (e.g. Dubner et al. 1990; Cappa et al. 1996; Vasquez et al. 2005; Giacani et al. 2011). In this scenario, the estimated dynamic age has to be attributed to the wind-blown shell. A similar scenario was suggested by Koo & Heiles (1995) to explain the detection of a high-velocity HI shell associated with the SNR W44.

4. Conclusions

We reported on the study of the radio counterpart of the newly discovered TeV source, HESS J1943+213. We analysed new and archival radio continuum data and archival HI spectral-line observations of the proposed radio counterpart, J1943+2118 (Abramowski et al. 2011).

Our high-resolution exploratory EVN observation provided the most accurate position of the source to date, thus strengthening the identification. From the EVN data, we could also calculate the brightness temperature of the source. The resulting low value indicates that relativistic beaming most probably does not play a role in the appearance of this source. According to the unified model of radio-loud AGNs (Urry & Padovani 1995), however, BL Lacertae objects are viewed at angles very close to the jet direction, therefore their radio emission is relativistically beamed, with apparent brightness temperatures well in excess of the equipartition value. Therefore, the measured low brightness temperature of J1943+2218 is not compatible with the BL Lacertae object nature, thus weakening the suggestion of Abramowski et al. (2011).

The re-analysed archival VLA C-array data, which recover emission at spatial scales that have been filtered out in the EVN observation, revealed an elongated source structure. Further radio observation at intermediate resolution is needed to better understand the radio structure of J1943+2218.

On the other hand, the HI data revealed a shell-like feature around J1943+2118. Even though we do not have yet an unequivocal evidence confirming that the two objects are associated, all the observed and derived parameters of this large-scale feature and the properties of the radio continuum source point to the discovery of a distant SNR whose PWN could be responsible for the TeV emission detected by H.E.S.S. If the HI shell is explained as a result of a SN explosion, then its dynamics indicate that the SN explosion took place $\sim 400\,000$ years ago. The X-ray to gamma-ray flux ratio on the other hand suggests a much younger ($\sim 10^3$ yrs) PWN. If the latter age is the correct, then the observed HI shell was not produced by the SN explosion but by the action of the stellar wind of the massive SN progenitor(s). Later the SN explosion took place within the rarefied wind cavity and the nebula created by its pulsar gave rise to the observed gamma-ray and X-ray emission. An ultimate evidence for the

PWN scenario would be the detection of pulsed radio emission from J1943+2118. It is worth mentioning that the SNR W44, a high energy gamma-ray emitter with an associated high-velocity HI shell, also harbours a pulsar (PSR B1853+01) which is powering a PWN (Frail et al. 1996).

The importance of the reported discovery resides not only in the fact that it naturally explains the nature of the TeV emission, but also, as remarked by Koo et al. (2006), it helps to solve the long-standing problem of the "missing" Galactic SNRs, where the detected SNRs barely make up 1% of the expected number.

Acknowledgements. We are grateful to the chair of the EVN Program Committee, Tiziana Venturi, for granting us short exploratory e-VLBI observing time in May 2011. The EVN is a joint facility of European, Chinese, South African, and other radio astronomy institutes funded by their national research councils. The NRAO is a facility of the National Science Foundation operated under cooperative agreement by Associated Universities, Inc. This work was supported by the European Community's Seventh Framework Programme, Advanced Radio Astronomy in Europe, grant agreement no. 227290, and Novel EXplorations Pushing Robust e-VLBI Services (NEXPReS), grant agreement no. RI261525. This research was supported by the Hungarian Scientific Research Fund (OTKA, grant no. K72515). GD and EG are members of CIC-CONICET (Argentina) and their work is partially supported by CONICET, ANPCYT and UBACYT grants from Argentina.

References

Abramowski, A., Acero, F., Aharonian, F., et al. 2011, A&A, 529, A49
Aharonian, F., Akhperjanian, A. G., Bazer-Bachi, A. R., et al. 2006, A&A, 457, 899
Cappa, C. E., Niemela, V. S., Herbstmeier, U., & Koribalski, B. 1996, A&A, 312, 283
Cioffi, D. F., McKee, C. F., & Bertschinger, E. 1988, ApJ, 334, 252
Condon, J. J., Cotton, W. D., Greisen, E. W., et al. 1998, AJ, 115, 1693
Cordes, J. M. & Lazio, T. J. W. 2002, ArXiv Astrophysics e-prints astro-ph/0207156
Dubner, G. M., Niemela, V. S., & Purton, C. R. 1990, AJ, 99, 857
Fey, A. L., Gordon, D., & Jacobs, C. S., eds. 2009, IERS Technical Note, Vol. 35
Fich, M., Blitz, L., & Stark, A. A. 1989, ApJ, 342, 272
Frail, D. A., Giacani, E. B., Goss, W. M., & Dubner, G. 1996, ApJ, 464, L165
Frey, S., Gurvits, L. I., Paragi, Z., & Gabányi, K. É. 2008, A&A, 484, L39
Gaensler, B. M. & Slane, P. O. 2006, ARA&A, 44, 17
Giacani, E., Smith, M. J. S., Dubner, G., & Loiseau, N. 2011, A&A, 531, A138
Kang, J., Koo, B.-C., & Salter, C. 2010, in Astronomical Society of the Pacific Conference Series, Vol. 438, The Dynamic Interstellar Medium: A Celebration of the Canadian Galactic Plane Survey, ed. R. Kothes, T. L. Landecker, & A. G. Willis, 372
Koo, B.-C. & Heiles, C. 1995, ApJ, 442, 679
Koo, B.-C., Kang, J.-H., & Salter, C. J. 2006, ApJ, 643, L49
Landi, R., Stephen, J. B., Masetti, N., et al. 2009, A&A, 493, 893
Maciel, W. J. & Quireza, C. 1999, A&A, 345, 629
Mattana, F., Falanga, M., Götz, D., et al. 2009, ApJ, 694, 12
Readhead, A. C. S. 1994, ApJ, 426, 51
Slane, P., Chen, Y., Schulz, N. S., et al. 2000, ApJ, 533, L29
Stil, J. M., Taylor, A. R., Dickey, J. M., et al. 2006, AJ, 132, 1158
Szomoru, A. 2008, in The role of VLBI in the Golden Age for Radio Astronomy, Proceedings of Science, PoS(IX EVN Symposium)040
Tomsick, J. A., Chaty, S., Rodriguez, J., Walter, R., & Kaaret, P. 2009, ApJ, 701, 811
Urry, C. M. & Padovani, P. 1995, PASP, 107, 803
Vasquez, J., Cappa, C., & McClure-Griffiths, N. M. 2005, MNRAS, 362, 681
Vollmer, B., Gassmann, B., Derrière, S., et al. 2010, A&A, 511, A53
Voskes, T. & Burton, W. B. 2006, ArXiv Astrophysics e-prints astro-ph/0601653